

Original Article  
Pharmacology



# Enhanced antibacterial activity of tilmicosin against *Staphylococcus aureus* small colony variants by chitosan oligosaccharide-sodium carboxymethyl cellulose composite nanogels

Wanhe Luo <sup>1,2</sup>, Jinhuan Liu <sup>1</sup>, Shanling Zhang <sup>1</sup>, Wei Song <sup>1</sup>,  
Samah Attia Algharib <sup>3</sup>, Wei Chen <sup>1,2,\*</sup>

<sup>1</sup>Engineering Laboratory for Tarim Animal Diseases Diagnosis and Control, College of Animal Science, Tarim University, Alar, Xinjiang 843300, China

<sup>2</sup>Key Laboratory of Tarim Animal Husbandry & Science Technology of Xinjiang Production & Construction Corps., Alar, Xinjiang 843300, China

<sup>3</sup>Department of Clinical Pathology, Faculty of Veterinary Medicine, Benha University, Moshtohor, Toukh 13736, QG, Egypt

 OPEN ACCESS

Received: Jul 20, 2021

Revised: Aug 17, 2021

Accepted: Oct 13, 2021

Published online: Nov 5, 2021

\*Corresponding author:

Wei Chen

Engineering Laboratory for Tarim Animal Diseases Diagnosis and Control/College of Animal Science, Tarim University, Key Laboratory of Tarim Animal Husbandry & Science Technology of Xinjiang Production & Construction Corps., Alar, Xinjiang 843300, China.

Email: 379497687@qq.com


© 2022 The Korean Society of Veterinary Science

This is an Open Access article distributed under the terms of the Creative Commons Attribution Non-Commercial License (<https://creativecommons.org/licenses/by-nc/4.0>) which permits unrestricted non-commercial use, distribution, and reproduction in any medium, provided the original work is properly cited.

ORCID iDs

Wanhe Luo 

<https://orcid.org/0000-0002-5170-1670>

Jinhuan Liu 

<https://orcid.org/0000-0001-6162-7534>

## ABSTRACT





**Background:** The poor bioadhesion capacity of tilmicosin resulting in treatment failure for *Staphylococcus aureus* small colony variants (SASCVs) mastitis.

**Objectives:** This study aimed to increase the bioadhesion capacity of tilmicosin for the SASCVs strain and improve the antibacterial effect of tilmicosin against cow mastitis caused by the SASCVs strain.

**Methods:** Tilmicosin-loaded chitosan oligosaccharide (COS)-sodium carboxymethyl cellulose (CMC) composite nanogels were formulated by an electrostatic interaction between COS (positive charge) and CMC (negative charge) using sodium tripolyphosphate (TPP) (ionic crosslinkers). The formation mechanism, structural characteristics, bioadhesion, and antibacterial activity of tilmicosin composite nanogels were studied systematically.

**Results:** The optimized formulation was comprised of 50 mg/mL (COS), 32 mg/mL (CMC), and 0.25 mg/mL (TPP). The size, encapsulation efficiency, loading capacity, polydispersity index, and zeta potential of the optimized tilmicosin composite nanogels were  $357.4 \pm 2.6$  nm,  $65.4 \pm 0.4\%$ ,  $21.9 \pm 0.4\%$ ,  $0.11 \pm 0.01$ , and  $-37.1 \pm 0.4$  mV, respectively; the sedimentation rate was one. Scanning electron microscopy showed that tilmicosin might be incorporated in nano-sized crosslinked polymeric networks. Moreover, adhesive studies suggested that tilmicosin composite nanogels could enhance the bioadhesion capacity of tilmicosin for the SASCVs strain. The inhibition zone of native tilmicosin, tilmicosin standard, and tilmicosin composite nanogels were  $2.13 \pm 0.07$ ,  $3.35 \pm 0.11$ , and  $1.46 \pm 0.04$  cm, respectively. The minimum inhibitory concentration of native tilmicosin, tilmicosin standard, and tilmicosin composite nanogels against the SASCVs strain were 2, 1, and 1  $\mu\text{g/mL}$ , respectively. The *in vitro* time-killing curves showed that the tilmicosin composite nanogels increased the antibacterial activity against the SASCVs strain.

**Conclusions:** This study provides a potential strategy for developing tilmicosin composite nanogels to treat cow mastitis caused by the SASCVs strain.

Shanling Zhang   
<https://orcid.org/0000-0002-6952-3972>  
Wei Song   
<https://orcid.org/0000-0001-5737-2583>  
Samah Attia Algharib   
<https://orcid.org/0000-0002-3336-2855>  
Wei Chen   
<https://orcid.org/0000-0003-2336-0108>

#### Funding

The study is financially supported by the President fund of Tarim University (TDZKSS202144), the Program for Young and Middle-aged Technology Innovation Leading Talents (2019CB029), the Program Nanjing Agricultural University-Tarim University Joint Fund (NNLH201901) to W. Chen and the Key Scientific and Technological Project of XPCC (2020AB025).

#### Conflict of Interest

The authors declare no conflicts of interest.

#### Author Contributions

Conceptualization: Luo W, Chen W; Data curation: Luo W, Liu J, Zhan S, Song W; Formal analysis: Luo W, Chen W; Funding acquisition: Chen W; Investigation: Luo W; Methodology: Luo W; Project administration: Chen W; Resources: Chen W; Software: Luo W; Supervision: Luo W; Validation: Luo W; Visualization: Luo W; Writing - original draft: Luo W, Liu J, Algharib SA; Writing - review & editing: Luo W, Liu J, Algharib SA.

**Keywords:** Tilmicosin; *Staphylococcus aureus*; nanogels; adhesives; mastitis

## INTRODUCTION

*Staphylococcus aureus* seriously threatens human health and results in substantial economic losses for livestock worldwide and has aroused considerable concern [1]. In particular, the presence of *Staphylococcus aureus* small colony variants (SASCVs) in the host cells could establish reservoirs from which reinfection can occur and result in long-term and repeated infection [2]. Because tilmicosin concentrates in the udder efficiently, it has been suggested to treat cow mastitis. The minimum inhibitory concentration (MIC) of tilmicosin against *S. aureus* isolated from cow mastitis was reported to be 2.2 µg/mL [3]. Tilmicosin was suggested to have strong antibacterial activity against SASCVs because of the strong antibacterial activity of tilmicosin against *S. aureus*. Thus, tilmicosin is a candidate drug for treating cow mastitis caused by SASCVs owing to its excellent pharmacodynamics (PD) and pharmacokinetics (PK). On the other hand, tilmicosin might be ineffective for SASCVs mastitis because of its inadequate therapeutic drug concentrations and insufficient residence time of the antibiotic in the mammary gland [4]. The therapeutic drug concentrations and residence time in the mammary gland could be increased by modifying the bioadhesive ability of tilmicosin to SASCVs [5]. Therefore, there is an urgent need to develop novel smart delivery systems to modify the bioadhesive ability of tilmicosin to SASCVs, increase the therapeutic drug concentrations and residence time in the mammary gland, and enhance the efficacy of tilmicosin against cow mastitis caused by SASCVs.

Nanogels (crosslinked polymeric networks) have the advantages of both nanoparticles and hydrogel [6]. They are used to incorporate more than one drug, have excellent structural stability and bioadhesion performance for bacteria [7]. Thus, nanogels might be effective delivery systems to improve the bioadhesion capacity of antibacterial agents and enhance their treatment against SASCVs. The bioadhesion capacity is mainly up to the mucoadhesive materials [8]. Some research has shown that gel materials have excellent bioadhesion capacity. For example, sodium carboxymethyl cellulose (CMC), as a polysaccharide carrier material, is commonly used to deliver drugs, proteins, and genes because of its non-toxicity, excellent biocompatibility, and biodegradable [9,10]. In addition, chitosan with a low molecular weight, called chitosan oligosaccharide (COS), which has a positive charge, better water-solubility, and antibacterial function, has been used in the nanogel drug delivery systems [11].

In the present study, novel smart delivery composite nanosystems were designed. The designed composite nanogels might improve the bioadhesion capacity of tilmicosin to SASCVs and enhance the antibacterial ability of antibacterial agents by COS-CMC composite nanogels (**Fig. 1**). The formation mechanism, structural characteristics, bioadhesion, and antibacterial activity of the tilmicosin composite nanogels were studied systematically.

## MATERIALS AND METHODS

### Materials

Tilmicosin solution and tilmicosin were obtained from ChuangXin Pharmaceutical Co., Ltd. (China) and Jinan Xinbao Star Animal Pharmaceutical Co., Ltd. (China), respectively. Tilmicosin standard was purchased from the China Institute of Veterinary Drugs Control

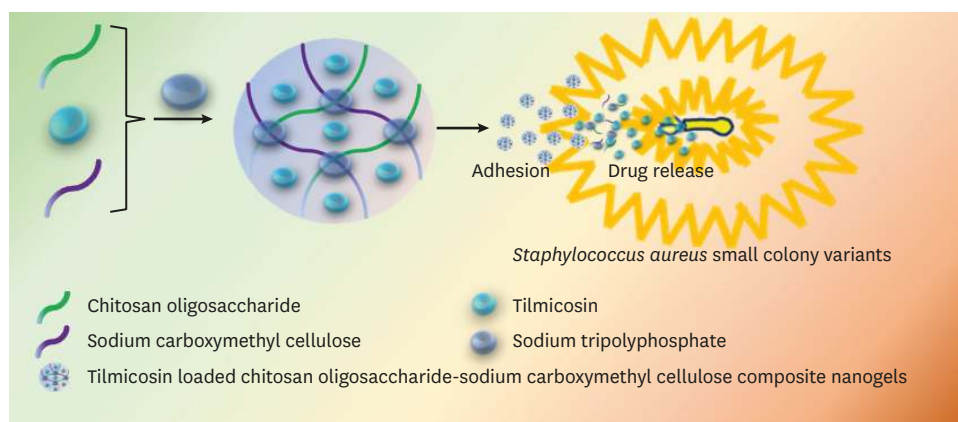


**Fig. 1.** Schematic diagram describing the synthesis of tilmicosin-loaded chitosan oligosaccharide-sodium carboxymethyl cellulose composite nanogels.

(China). COS, CMC, and TPP were obtained from Tada Gene Co. Ltd (China). The SASCVs strain was obtained from the Engineering Laboratory for Tarim Animal Diseases Diagnosis and Control of Tarim University (China). The water was prepared using a Milli-Q system (Millipore, USA). The other reagents in the text were of analytical grade or equivalent.

### Quantitative measurement

The tilmicosin concentration was detected using a Waters 2695 series reverse-phase high-performance liquid chromatography (HPLC). A Symmetry<sup>®</sup> C<sub>18</sub> column (250 mm × 4.6 mm i.d., 5 μm) was used for separation. The mobile phase was 0.1 mol/L ammonium formate, acetonitrile, and methyl alcohol at 61: 29: 10 proportions. The standard curves of tilmicosin ranged from 0.05 to 100 μg/mL,  $R^2 = 0.9988$  with a recovery rate > 87% and relative standard deviations below 7.5% for the intra-day and inter-day variation. The specificity of the method was good for the target substances without endogenous interference on the chromatograms.

### Formulation of tilmicosin loaded COS-CMC composite nanogels

The tilmicosin-loaded COS-CMC composite nanogels were formulated by electrostatic interactions using an ionic crosslinker. Briefly, CMC (600, 800, or 1000 mg) were added to 15 mL of ultrapure water with magnetic stirring for complete dissolution. Subsequently, 0.4 mL of TPP (0.25 mg/mL) was added dropwise to the CMC solution with magnetic stirring at 1200 RPM. Concurrently, COS (300, 450, 600, 750, or 900 mg) was dissolved in 25 mL of ultrapure water. Ten milliliters of absolute alcohol containing 600 mg tilmicosin was added to the 25 mL COS solution at 0.5 mL/min under magnetic stirring. Finally, the COS solution mixture was added dropwise to the CMC mixture solution under magnetic stirring at 1,200 RPM to form the tilmicosin-loaded COS-CMC composite nanogels. The optimal amounts of CMC and CSO were evaluated by the loading capacity (LC) and encapsulation efficiency (EE). Briefly, different tilmicosin-loaded COS-CMC composite nanogels were centrifuged at 14,000 RPM for 60 min. The tilmicosin in the supernatant was then measured by HPLC to calculate the EE. The precipitate was lyophilized into a powder after re-suspending to calculate the LC. Each sample was formulated three times. The data are expressed as the mean ± SD.

### Characterization of the optimal tilmicosin loaded COS-CMC composite nanogels

#### Surface morphology determination

The appearance and optical microscopy images of the optimal tilmicosin-loaded COS-CMC composite nanogels were observed. The optimal tilmicosin composite nanogels were freeze-

dried using a lyophilizer and characterized by optical microscopy. The optimal tilmicosin composite nanogels were then evaluated by scanning electron microscopy (SEM). Briefly, 1 mg tilmicosin composite nanogels was suspended in 1 mL of distilled water, and 2  $\mu$ L of the suspension was placed on a coverslip. The samples were coated with gold by ion sputtering and examined at an accelerating voltage of 20 kV after oven-drying.

#### *Detection of the particle diameter, zeta potential (ZP), and polydispersity index (PDI)*

The particle diameter, ZP, and PDI of the optimal tilmicosin-loaded COS-CMC composite nanogels were measured using Zeta sizer ZX3600. Before the test, the tilmicosin composite nanogels were appropriately diluted to obtain the optimal kilo counts per second.

#### *Determination of sedimentation rate (F)*

The original height ( $H_0$ ) of the 30 mL tilmicosin nanogels sample in a 100 mL graduated cylinder after shaking was measured. The height (H) of the sediment in the cylinder after standing for 3 h was recorded. F was calculated using the equation,  $F = H/H_0$ .

#### *In vitro release*

The optimal tilmicosin-loaded COS-CMC composite nanogels were added to a dialysis bag that was then placed into 500 mL phosphate-buffered saline (PBS, pH 6.5 and 7.4) at  $37 \pm 0.5^\circ\text{C}$  after sealing. At different time points (0.5, 1, 2, 3, 4, 6, 8, 12, 24, 36, and 48 h), 1 mL of the dialysate was removed, and HPLC measured the drug concentration. Subsequently, the cumulative release percentage was calculated, and the cumulative release curve was plotted.

### **Mucoadhesive studies**

The tilmicosin composite nanogels were placed into a liquid medium containing the SASCVs strain of the logarithmic growth phase of  $10^6$  CFU/mL at the final tilmicosin concentrations of 10  $\mu\text{g/mL}$ . The liquid culture was drawn on the copper mesh after incubation for 30 min. SEM was performed to determine if the tilmicosin composite nanogels were adsorbed on the bacteria surface.

### **Antibacterial activity studies**

#### *The disk diffusion test*

The agar diffusion method was used to estimate the *in vitro* antibacterial activity of native tilmicosin, tilmicosin standard, and tilmicosin composite nanogels. Briefly, 15 mL of agar medium was first poured into an aseptic plate. Once the agar had solidified, another 5 mL agar medium containing 0.1 mL of bacterial fluid (contained  $10^5$ – $10^6$  CFU SASCVs strain) was poured over the 15 mL agar medium. When the agar was solid, four holes in the solid agar were made using a straw. Subsequently, 50  $\mu$ L physiological saline, tilmicosin standard, native tilmicosin, and composite nanogels (tilmicosin content: 10  $\mu\text{g/mL}$ ) were added. Physiological saline was used as the control. The plates incubating the SASCVs strain were placed in an incubator (5%  $\text{CO}_2$ ,  $37^\circ\text{C}$ ) for 24 h, and the size of the inhibition zones was measured and recorded.

#### *Broth macrodilution method*

The antibacterial activity of native tilmicosin, tilmicosin standard, and tilmicosin composite nanogels was studied using the broth macrodilution method, as recommended by the Clinical and Laboratory Standards Institute (CLSI). Briefly, serial dilutions of the three different tilmicosin formulations in Mueller-Hinton broth were prepared. Subsequently, the SASCVs strain was added to each tube to achieve a final inoculum of  $1 \times 10^5$  CFU/mL. The

minimum inhibitory concentration of tilmicosin was defined as the lowest concentration inhibiting the visible growth of bacteria after 24 h incubation of the cultures at 37°C.

#### Time-killing curves

The *in vitro* killing curves of native tilmicosin, tilmicosin standard, and tilmicosin composite nanogels against SASCVs strain were obtained by plotting time as a function of  $\log_{10}$  CFU/mL. The SASCVs strain was added to 2 ml of MH broth, giving a starting inoculum of  $10^6$  CFU/mL. The native tilmicosin, tilmicosin standard, and tilmicosin composite nanogels were added to obtain a serial concentration corresponding to  $1/2 \times \text{MIC}$ ,  $1 \times \text{MIC}$ ,  $2 \times \text{MIC}$ ,  $4 \times \text{MIC}$ ,  $8 \times \text{MIC}$ , and  $16 \times \text{MIC}$ . The tubes were placed at 37°C, and the bacterial count (CFU/mL) was determined using the agar dilution method for each tube after incubating for 1, 2, 4, 8, 12, 24, 48, and 72 h. Briefly, 10-fold serial dilutions from each culture sample were performed, and 100  $\mu\text{L}$  of each dilution was then spread over the agar plates and incubated at 37°C. The viable colonies were then counted after 24 h. Each concentration was performed in triplicate. The limit of detection was 10 CFU/mL [5].

#### Statistical analysis

The experimental data are expressed as the mean  $\pm$  SD and analyzed by one-way analysis of variance using SPSS software; *p* values < 0.05 were considered significant.

## RESULTS

#### Optimization of tilmicosin-loaded COS-CMC composite nanogels

Tilmicosin-loaded COS-CMC composite nanogels were formulated by electrostatic interactions between COS (positive charge) and CMC (negative charge) using TPP (crosslinkers). The amount of COS and CMC were chosen as variables. LC and EE are the crucial parameters as far as the formulation of drugs are significant. Thus, the tilmicosin composite nanogels were optimized by a single factor test using EE and LC as the assessment indices. The amount of COS and CMC affected the mean LC and EE of tilmicosin composite nanogels considerably (Table 1). The optimal tilmicosin-loaded COS-CMC composite nanogels were obtained when the EE and LC of the composite nanogels were the largest. The mean LC and EE of the optimal tilmicosin-loaded COS-CMC composite nanogels was  $21.9\% \pm 0.4\%$  and  $65.4\% \pm 0.4\%$ . Hence, the final optimal formula was comprised of 50 mg/mL (COS) and 32 mg/mL (CMC).

#### Properties of the tilmicosin composite nanogels

The tilmicosin-loaded COS-CMC composite nanogels had the appearance of a homogenous canary yellow uniform suspension with a sedimentation rate of 1 (Fig. 2A). After the tilmicosin-loaded COS-CMC composite nanogels were freeze-dried using a lyophilizer, the lyophilized nanogels exhibited a uniform cross-linked polymeric network (Fig. 2B). Optical microscopy

**Table 1.** Optimization of tilmicosin-loaded COS-CMC composite nanogels (Mean  $\pm$  SD, *n* = 3)

Serial number	COS (mg/mL)	CMC (mg/mL)	TPP (mg/mL)	LC (%)	EE (%)
1	20	32	0.25	9.3 $\pm$ 0.4	47.5 $\pm$ 0.5
2	30	32	0.25	11.7 $\pm$ 0.6	50.7 $\pm$ 0.4
3	40	32	0.25	15.2 $\pm$ 0.6	54.5 $\pm$ 0.7
4	50	32	0.25	21.9 $\pm$ 0.4	65.4 $\pm$ 0.4
5	60	32	0.25	20.5 $\pm$ 0.4	63.3 $\pm$ 0.3
6	50	24	0.25	19.0 $\pm$ 0.5	60.8 $\pm$ 0.5
7	50	40	0.25	18.2 $\pm$ 0.2	58.6 $\pm$ 0.3

COS, chitosan oligosaccharide; CMC, sodium carboxymethyl cellulose; TPP, sodium tripolyphosphate; EE, loading capacity; LC, encapsulation efficiency.

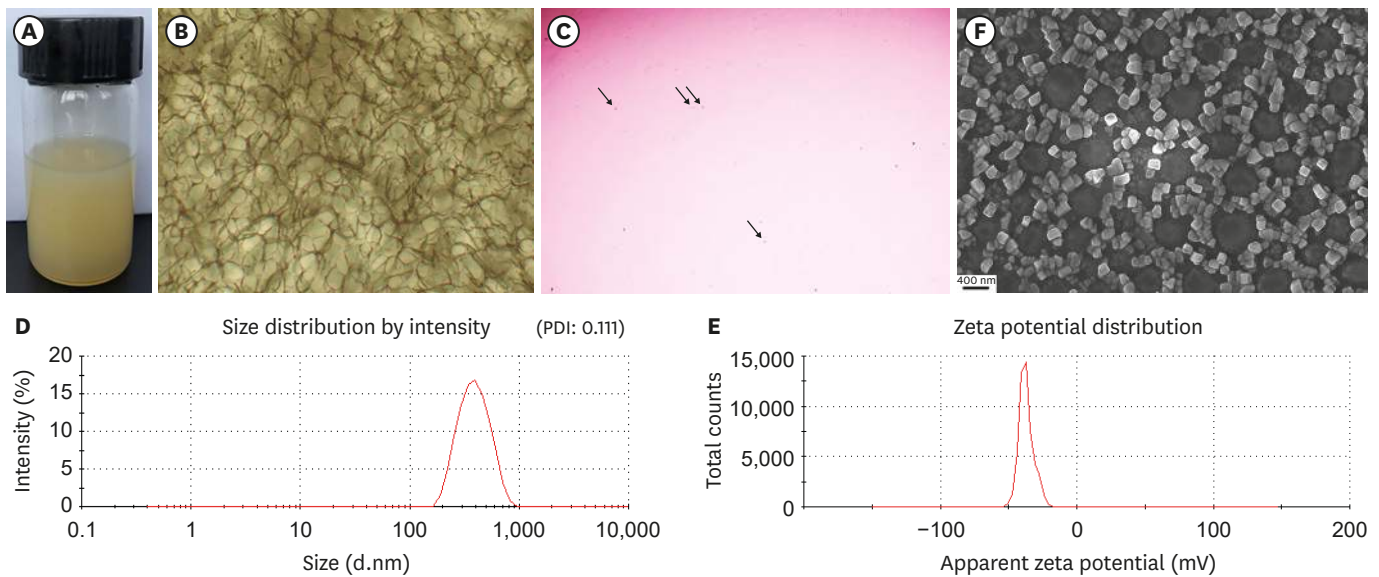


**Fig. 2.** Properties of the optimal tilmicosin-loaded chitosan oligosaccharide-sodium carboxymethyl cellulose composite nanogels. (A) appearance, (B) lyophilized nanogels by light microscope (Magnification  $\times 40$ ), (C) fresh nanogels by light microscope (Magnification  $\times 100$ ), (D) size distribution, (E) Zeta potential, (F) SEM images. PDI, polydispersity index.

showed that the tilmicosin composite nanogels were well dispersed with good particle size distributions and a spherical shape (**Fig. 2C**). The mean sizes, PDI, and ZP of the optimal tilmicosin composite were  $357.4 \pm 2.6$  nm (**Fig. 2D**),  $0.11 \pm 0.01$ , and  $-37.1 \pm 0.4$  mV (**Fig. 2E**), respectively. SEM revealed a nano-sized crosslinked polymeric network (**Fig. 2F**). This may be due to the electrostatic interactions between COS and CMC with the help of TPP. More importantly, tilmicosin might be incorporated in the nano-sized crosslinked polymeric networks. After the tilmicosin-loaded COS-CMC composite nanogels were lyophilized, the image also revealed crosslinked polymeric networks. Thus, the tilmicosin-loaded COS-CMC composite nanogel was prepared successfully by electrostatic interactions using an ionic crosslinker.

### **In vitro release study**

Considering that the pH of *S. aureus* infection sites (mammary gland) is usually 6.5 and the pH of mammary gland cells is 7.4 [12], the release of the tilmicosin-loaded COS-CMC composite nanogels in pH 6.5 and 7.4 were measured to determine the environmental pH-responsive release. At pH 6.5,  $44.5\% \pm 1.1\%$  was released from the tilmicosin-loaded COS-CMC composite nanogels at 48 h, while  $36.8\% \pm 2.1\%$  was released in the pH 7.4 PBS at 48 h (**Fig. 3**). These results suggest that the designed composite nanogels at both pHs exhibited prominent sustained-release performance.

### **Adhesive studies**

The co-culture of SASCVs and tilmicosin-loaded COS-CMC composite nanogels for 30 min were observed by SEM. SEM showed that the tilmicosin composite nanogels were in contact with or absorbed on the SASCVs strains (**Fig. 4**). A large number of tilmicosin-loaded COS-CMC composite nanogels were in contact with or absorbed on the surface of SASCVs strains (**Fig. 4A**). On the other hand, the tilmicosin solution was not or rarely in contact with or absorbed on the surface of the SASCVs strains (**Fig. 4B**). Thus, the designed composite nanogels might improve the bioadhesion capacity of tilmicosin to the SASCVs and enhance the treatment effects of tilmicosin against SASCVs infections.

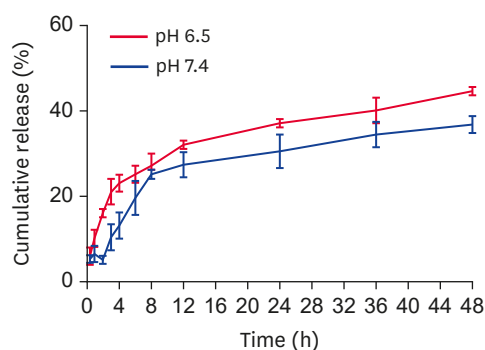


**Fig. 3.** The cumulative release of tilmicosin-loaded chitosan oligosaccharide-sodium carboxymethyl cellulose composite nanogels in pH 6.5 and 7.4 PBS (Mean  $\pm$  SD, n = 3).

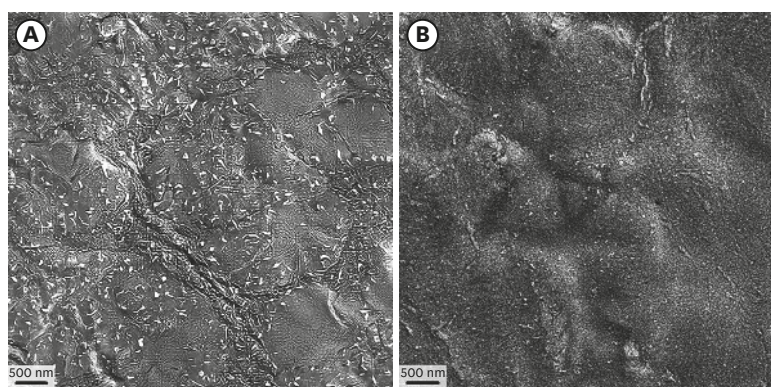


**Fig. 4.** Scanning electron microscopy images of co-culture of *Staphylococcus aureus* small colony variants strain and tilmicosin-loaded chitosan oligosaccharide-sodium carboxymethyl cellulose composite nanogels (A) and tilmicosin solution (B) for 30 min.

### Antibacterial activity test *in vitro*

**Fig. 5** shows the antibacterial activity of native tilmicosin, tilmicosin standard, and tilmicosin-loaded COS-CMC composite nanogels. From the size of the inhibition zone, the tilmicosin composite nanogels exhibited excellent antibacterial activity against the SASCVs strain. The inhibition zone of the control, native tilmicosin, tilmicosin standard, and tilmicosin composite nanogels were 0.0 cm,  $2.13 \pm 0.07$  cm,  $3.35 \pm 0.11$  cm, and  $1.46 \pm 0.04$  cm, respectively (**Fig. 5A**). The MICs of native tilmicosin, tilmicosin standard, and tilmicosin composite nanogels against the SASCVs strain were  $2 \mu\text{g/mL}$ ,  $1 \mu\text{g/mL}$ , and  $1 \mu\text{g/mL}$ , respectively. *In vitro* time-killing curves of native tilmicosin, tilmicosin standard, and tilmicosin composite nanogels against SASCVs strain were illustrated in **Fig. 5B-D**. According to these profiles, native tilmicosin, tilmicosin standard, and tilmicosin composite nanogels showed a concentration-dependent bactericidal effect as increasing the drug concentrations induced swifter and more radical killing effects. The bactericidal effect of tilmicosin was observed when the concentration of native tilmicosin, tilmicosin standard, and tilmicosin composite nanogels were  $2 \times \text{MIC}$  ( $4 \mu\text{g/mL}$ ,  $2 \mu\text{g/mL}$ , and  $2 \mu\text{g/mL}$ ). With increasing tilmicosin concentration, obvious inhibition of bacterial growth was observed in a very short period. Hence, the bactericidal activity increased with increasing drug concentration.

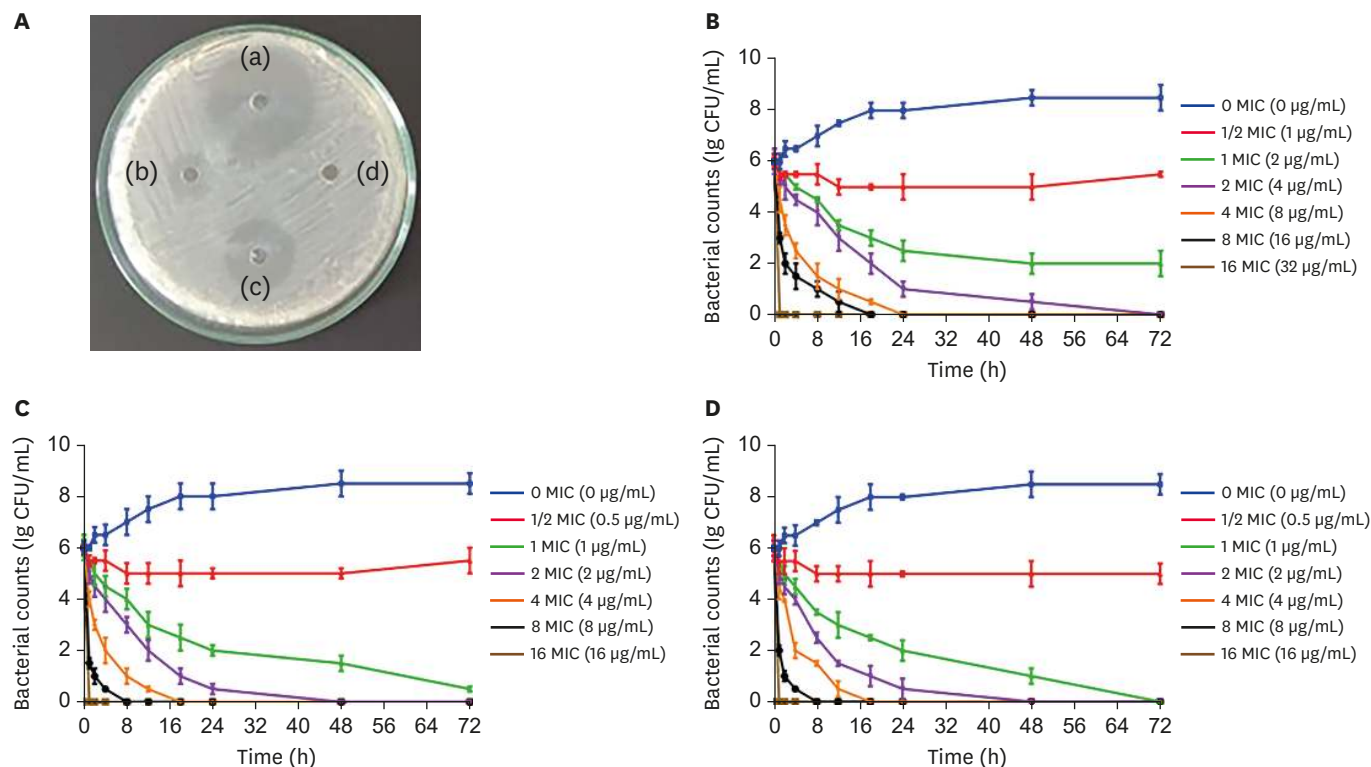


**Fig. 5.** Antibacterial activity of different tilmicosin formulations against the SASCVs strain. (A) the inhibition zones of tilmicosin standard (a), tilmicosin composite nanogels (b), native tilmicosin (c), and physiological saline (d). (B) the killing curve of native tilmicosin, (C) tilmicosin standard, and (D) tilmicosin composite nanogels against SASCVs strain (n = 3). SASCVs = *Staphylococcus aureus* small colony variants.

## DISCUSSION

Combining the merits of nanoparticles and hydrogels to prepare composite nanogels to enhance the bioadhesion capacity of antibacterial drugs to bacteria and increase the therapeutic drug concentration and efficacy of antibacterial drugs against bacteria has attracted considerable interest [13,14]. In this study, tilmicosin-loaded COS-CMC composite nanogels were formulated by electrostatic interactions between COS (positive charge) and CMC (negative charge) using TPP (ionic crosslinkers). The COS and CMC concentrations were selected as variables to optimize the tilmicosin-loaded loaded COS-CMC composite nanogels by a single factor test using EE and LC as assessment indices. The formation of tilmicosin composite nanogels was more successful when the EE and LC of tilmicosin-loaded COS-CMC composite nanogels were greater. Therefore, the final optimal formula was comprised of 50 mg/mL (COS), 32 mg/mL (CMC), and 0.25 mg/mL (TPP). Optical microscopy showed that the tilmicosin composite nanogels were well dispersed with good particle size distributions and a spherical shape, which agrees with previous studies [2]. The appearance of lyophilized nanogels showed a uniform crosslinked polymeric network. Moreover, SEM showed that tilmicosin might be incorporated in nano-sized crosslinked polymeric networks, suggesting that tilmicosin-loaded COS-CMC composite nanogels had been formulated successfully by electrostatic interactions between COS and CMC using TPP. This result is consistent with the schematic diagram of tilmicosin-loaded COS-CMC composite nanogels. On the other hand, the particle size of the tilmicosin-loaded loaded COS-CMC composite nanogels detected by SEM was smaller than that determined using the



Zeta sizer ZX3600. The difference might be because the particle size was tested using a Zeta sizer ZX3600 in the aqueous state. Free water and some hydrated water were evaporated, so the size measured by the Zeta sizer was usually larger than the real size. On the other hand, the particle sizes measured by SEM were smaller than the genuine diameters. This result is consistent with previous studies [5].

For nanogels, the drug is dispersed/dissolved uniformly in the matrix. Hence, release occurs mainly by a combination of drug diffusion, polymer swelling, surface, and bulk erosion of the matrix. In the *in vitro* release study,  $44.5\% \pm 1.1\%$  and  $36.8\% \pm 2.1\%$  tilmicosin were released from the tilmicosin-loaded COS-CMC composite nanogels in the pH 6.5 and 7.4 PBS at 48 h, respectively. Thus, the *in vitro* release study indicated that the tilmicosin-loaded COS-CMC composite nanogels at both pH (6.5 and 7.4) had prominent sustained-release performance and might be delivered effectively to the mammary gland in the intact state. The co-culture of SASCVs strain and tilmicosin-loaded COS-CMC composite nanogels and tilmicosin solution for 30 min was observed by SEM to determine if the bioadhesion capacity of tilmicosin to bacteria was enhanced. A large number of tilmicosin-loaded COS-CMC composite nanogels were contacted with or absorbed on the surface of the SASCVs strains, but a tilmicosin solution was not or rarely contacted with or absorbed on the surface of SASCVs strains. These results suggest that the tilmicosin composite nanogels might enhance the bioadhesion capacity of tilmicosin to the SASCVs strain because the cationic nature of COS interacts with the negative charge of SASCVs strain and the excellent adhesion of CMC. This might influence the integrity of bacterial cell membranes or increase the drugs accessing bacteria, hence, increase the antibacterial activity of tilmicosin.

*In vitro* antibacterial tests were performed to determine if the tilmicosin composite nanogels could improve the *in vitro* antibacterial activity of tilmicosin, compare the antibacterial activity of the nanogel with the commercial preparation, and determine if the preparation methods affect the antibacterial activity of tilmicosin. The disk diffusion test showed that the tilmicosin composite nanogels did not improve the antibacterial activity of tilmicosin *in vitro*, and the antibacterial activity was slightly weak compared to commercial preparations. On the other hand, the MIC of native tilmicosin, tilmicosin standard, and tilmicosin composite nanogels against SASCVs strain showed that the tilmicosin composite nanogels improve the antibacterial activity of tilmicosin *in vitro* compared to commercial preparations. This might be because the diffusion of the tilmicosin composite nanogels in agar was more difficult than the tilmicosin solution, but the diffusion of the tilmicosin composite nanogels in the Mueller-Hinton broth was easier. Although the *in vitro* antibacterial activity of tilmicosin was not improved, the MIC of the tilmicosin standard and tilmicosin composite nanogels was similar. This suggests that the structure of tilmicosin was not changed in the process of preparing the tilmicosin composite nanogels. For the time-killing curves, tilmicosin composite nanogels displayed more effective bactericidal activity against the SASCVs strain than the tilmicosin standard, particularly native tilmicosin. The native tilmicosin, tilmicosin standard, and tilmicosin composite nanogels exhibited bactericidal activity against the SASCVs strain, demonstrating that tilmicosin is concentration-dependent. Thus, the area under concentration-time curve/minimum inhibitory concentration (AUC/MIC) might be the most appropriate parameter to formulate the dosage regimen of the three different preparations of tilmicosin against cow mastitis caused by the SASCVs strain because of their concentration-dependent bactericidal effect. The tilmicosin composite nanogels could fully inhibit the SASCVs strain. This might be because the designed composite nanogels could be more effective in modifying the bioadhesive ability of tilmicosin to the SASCVs strain,

thus displaying a stronger curative effect. These results suggest that tilmicosin composite nanogels might be a potential strategy to solve the therapy difficulty of cow mastitis caused by SASCVs strains.

Tilmicosin-loaded COS-CMC composite nanogels were successfully formulated by an electrostatic interaction between COS (positive charge) and CMC (negative charge) using TPP (ionic crosslinkers) to enhance the efficacy of tilmicosin against cow mastitis caused by the SASCVs strain. The tilmicosin-loaded COS-CMC composite nanogels were a homogenous canary yellow uniform suspension with a sedimentation rate of one. Tilmicosin was incorporated in nano-sized crosslinked polymeric networks, and particle size distributions of  $357.4 \pm 2.6$  nm, PDI of  $0.11 \pm 0.01$ , ZP of  $-37.1 \pm 0.4$  mV, EE of  $65.4\% \pm 0.4\%$ , LC of  $21.9\% \pm 0.4\%$ , and a sedimentation rate of one. More importantly, the tilmicosin-loaded COS-CMC composite nanogels could enhance the bioadhesion capacity of tilmicosin to the SASCVs strain. Furthermore, the tilmicosin composite nanogels displayed more effective bactericidal activity against SASCVs strain than the tilmicosin standard, especially native tilmicosin. Therefore, the prepared tilmicosin composite nanogels might help solve the therapeutic difficulty of cow mastitis caused by SASCVs strains.

## REFERENCES

1. Zhou K, Li C, Chen D, Pan Y, Tao Y, Qu W, et al. A review on nanosystems as an effective approach against infections of *Staphylococcus aureus*. *Int J Nanomedicine*. 2018;13:7333-7347.  
[PUBMED](#) | [CROSSREF](#)
2. Algharib SA, Dawood A, Zhou K, Chen D, Li C, Meng K, et al. Designing, structural determination and biological effects of rifaximin loaded chitosan- carboxymethyl chitosan nanogel. *Carbohydr Polym*. 2020;248:116782.  
[PUBMED](#) | [CROSSREF](#)
3. Wang XF, Zhang SL, Zhu LY, Xie SY, Dong Z, Wang Y, et al. Enhancement of antibacterial activity of tilmicosin against *Staphylococcus aureus* by solid lipid nanoparticles *in vitro* and *in vivo*. *Vet J*. 2012;191(1):115-120.  
[PUBMED](#) | [CROSSREF](#)
4. Zhou K, Wang X, Chen D, Yuan Y, Wang S, Li C, et al. Enhanced treatment effects of tilmicosin against *Staphylococcus aureus* cow mastitis by self-assembly sodium alginate-chitosan nanogel. *Pharmaceutics*. 2019;11(10):524.  
[PUBMED](#) | [CROSSREF](#)
5. Liu Y, Chen D, Zhang A, Xiao M, Li Z, Luo W, et al. Composite inclusion complexes containing hyaluronic acid/chitosan nanosystems for dual responsive enrofloxacin release. *Carbohydr Polym*. 2021;252:117162.  
[PUBMED](#) | [CROSSREF](#)
6. Shu M, Long S, Huang Y, Li D, Li H, Li X. High strength and antibacterial polyelectrolyte complex CS/HS hydrogel films for wound healing. *Soft Matter*. 2019;15(38):7686-7694.  
[PUBMED](#) | [CROSSREF](#)
7. Cao J, Wu P, Cheng Q, He C, Chen Y, Zhou J. Ultrafast fabrication of self-healing and injectable carboxymethyl chitosan hydrogel dressing for wound healing. *ACS Appl Mater Interfaces*. 2021;13(20):24095-24105.  
[PUBMED](#) | [CROSSREF](#)
8. Yang Z, Huang R, Zheng B, Guo W, Li C, He W, et al. Highly stretchable, adhesive, biocompatible, and antibacterial hydrogel dressings for wound healing. *Adv Sci (Weinh)*. 2021;8(8):2003627.  
[PUBMED](#) | [CROSSREF](#)
9. Yang HN, Park JS, Jeon SY, Park KH. Carboxymethylcellulose (CMC) formed nanogels with branched poly(ethyleneimine) (bPEI) for inhibition of cytotoxicity in human MSCs as a gene delivery vehicles. *Carbohydr Polym*. 2015;122:265-275.  
[PUBMED](#) | [CROSSREF](#)
10. Zhu K, Ye T, Liu J, Peng Z, Xu S, Lei J, et al. Nanogels fabricated by lysozyme and sodium carboxymethyl cellulose for 5-fluorouracil controlled release. *Int J Pharm*. 2013;441(1-2):721-727.  
[PUBMED](#) | [CROSSREF](#)

11. Liu L, Xu Y, Zhang P, You J, Li W, Chen Y, et al. High-order assembly toward polysaccharide-based complex coacervate nanodroplets capable of targeting cancer cells. *Langmuir*. 2020;36(29):8580-8588.  
[PUBMED](#) | [CROSSREF](#)
12. Marshall MO, Knudsen J. Biosynthesis of triacylglycerols containing short-chain fatty acids in lactating cow mammary gland. Activity of diacylglycerol acyltransferase towards short-chain acyl-CoA esters. *Eur J Biochem*. 1977;81(2):259-266.  
[PUBMED](#) | [CROSSREF](#)
13. Peng H, Huang X, Melle A, Karperien M, Pich A. Redox-responsive degradable prodrug nanogels for intracellular drug delivery by crosslinking of amine-functionalized poly(N-vinylpyrrolidone) copolymers. *J Colloid Interface Sci*. 2019;540:612-622.  
[PUBMED](#) | [CROSSREF](#)
14. Algharib SA, Dawood A, Xie S. Nanoparticles for treatment of bovine *Staphylococcus aureus* mastitis. *Drug Deliv*. 2020;27(1):292-308.  
[PUBMED](#) | [CROSSREF](#)